

Comparison of Artificial Neural Networks and Autoregressive Model to Forecast Inflows to Roseires Reservoir for better Prediction of Irrigation Water Supply in the Sudan

Mawada E. Abdellatif¹, Yassin Z. Osman², Adil M. Elkhidir³

¹School of the Built Environment, Liverpool John Moores University, Byrom Street, Liverpool, L3 3AF, UK

E-mail: M.E.Abdellatif@ljmu.ac.uk (Corresponding author)

²Faculty of Advanced Engineering, University of Bolton, Deane Road, Bolton, BL3 5AB, UK.

³Department of Civil Engineering, Faculty of Engineering & Architecture, University of Khartoum, Khartoum, Sudan

E-mail: M.E.Abdellatif@ljmu.ac.uk (Corresponding author)

Abstract

The Blue Nile River is utilised in the Sudan as main source of irrigation water. However, the river has a long dry low flow season (October to May), which necessitates use of regulations and rules to manage its water use during this period. This depends on use of accurate lead time forecasts of inflows to the reservoirs built along the river. Thus a reliable and tested forecasting tool is needed to provide inflow forecast, with sufficient lead time. In the present study Artificial Neural Network (ANN) is used to model the recession curve of the flow hydrograph at El-Deim gauging station which subsequently used as inflows to the Roseires Reservoir on the Blue Nile River. Different scenarios of ANN have been tested to forecast 23 10-day mean discharges during the recession period and their performances were assessed. Results from the optimal ANN model were compared to those simulated with an autoregressive (AR1) model to check their accuracy. Modelling results showed that the ANN model developed is capable of accurately forecasting the inflows to the Roseires Reservoir and outperform the AR1 model and. It has then proposed for use in operation of the reservoir for purposes of predicting irrigation water supply.

Key words: Artificial neural network, Autoregressive model, Recession curve, Blue Nile River, El Deim, NeuroShell2

1. Introduction

The Blue Nile River flows out of Lake Tana in the Ethiopian plateau at an altitude of 850m, and pass through gorges until reaches the Sudan plains at an elevation of 500m. It then flows in a northern westerly direction to its confluence with the White Nile at Khartoum (see Fig. 1). The most upstream gauging station on the Blue Nile River reach in the Sudan is El-Deim station and the most downstream gauging one is at Khartoum. The Blue Nile flows undergo rapid variability during flooding season, so understanding the exact behaviour of this river is necessary for effective management of its water.

. Two reservoirs have been constructed along the river reach in the Sudan to best utilise its water; these are Sennar and Roseires reservoirs. The Blue Nile Water System, including the Sennar and Roseires reservoirs, is operated with document “Regulation Rules for the Working of the Reservoirs”, which is prepared by the Ministry of irrigation and Water Resources in 1968 (Sughaiyaroun, 1968). The aim of the rules is to distribute

stored water and natural river flow for irrigation schemes and maintain minimum flows at Khartoum. The rules consider the hydrological or water year to begin on the first of June and ends on the 31th of May (cf. Fig. 2 below); and give priority for the requirements of irrigation over the requirements for power generation.

Fig. 2 shows a typical flow hydrograph at El-Deim gauging station for the water year 1976/1977. The flow in Fig. 2 is given as 10-day mean discharge (in million cubic metres per day, (Million m³/day)), which is a quantitative measuring concept used by the Ministry of Irrigation in the Sudan to assess water volume in the Blue Nile for storage purposes. It is obtained by taking the average of the 10 preceding daily discharges. Therefore, there are 3 data points of 10-day mean discharge in each month (e.g. Q1Jun stands for period 01/06 to 10/06, Q2Jun stands for period 11/06 – 20/06, and Q3Jun stands for period 21/06 – 30/06) and 36 data points in a water year, which extends from 1st June of a calendar year and finishing at 31st May of the following calendar year (see Fig. 02). From the 10-day mean discharge, a 10-day volume can be obtained by multiplying the discharge by 10 days to obtain a water volume in million cubic metres. Therefore, there are also 3 data points of 10-day volume in a month (e.g. V1Jun, V2Jun, and V3Jun) and 36 data points in a water year.

The irrigation needs and operation of the two reservoirs depend mainly on the flow pattern of the river in the dry season period (recession period) from October to May after the high flow passes as depicted in Fig. 2. During this recession period demands usually exceed the water supplied by the river. Therefore, the main objective of this paper is to build a model to give a lead time forecast (weeks to months in advance) of inflows to the Roseires Reservoir from El-Deim gauging station during the dry season or recession period in the Blue Nile flows. This lead time forecast can subsequently be used to determine the amount of storage in the reservoir and water available for irrigation and hence the area to be cultivated.

Different prediction methods have been used to forecast inflows to the Roseires Reservoir from El-Deim station. The Ministry of Irrigation in the Sudan uses a graphical method to predict outflows of El-Deim station during the dry season. The method consists of drawing different hydrographs for past characteristic years and then entering the actual flows of the specific year from first ten day period of June to first ten days period of October in the same hydrograph (i.e. Q1Jun, Q1Jul, Q1Aug, Q1Sep and Q1Oct) and then read the corresponding 10-day discharges from the 2nd period of October (Q2Oct) to the 3rd period of May (Q3May), based on pattern of the hydrographs in the past years. The hydrographs used in the graphical method are those for years 1913, 1972, and 1984. Thus, as an approximate procedure, the graphical method sometimes gives reasonable forecast; other time gives inaccurate forecast and hence can result in mismanagement of water. However, beside forecast accuracy the main problem with the graphical method is absence of sufficient lead time for the forecast as it is required to wait until the first ten days period of October in the water year in order to get a forecast for the second ten days of October in the same water year (a maximum of 10 days lead time). Therefore, the main objective of the present study to develop an accurate and reliable model to forecast inflows to the Roseires Reservoir, during the recession period, with sufficient lead time forecast. Having accurate forecast with sufficient lead time would lead definitely to improvement in the water management of the reservoir in estimating water supply for irrigation purposes.

Artificial Neural Network (ANN) models, which used in this study, have recently been successfully used in hydrological forecasting field. Many studies have demonstrated that ANN models are very successful in simulating river flows (e.g. Shamseldin (1997); Coulibaly et al. (2000); Chang & Chen (2001); Dibike & Solomatine (2001); Shamseldin et al. (2002) & (2007); Rajurkar et al. (2004); Dawson et al. (2006); Abrahart et al. (2007); Boucher et al. (2009); Pramanik & Panda (2009); and Shamseldin (2010)) and hence they are worthy of investigation with regard to forecast inflow to the Roseires Reservoir on the Blue Nile. Moreover, previous success stories of using ANN models in the Blue Nile river flow forecasting (e.g. Antar et al. (2005) and Shamseldin (2010)) formed great motivation to use the method in the present study. However, unlike those studies, in which the ANN models have been used in the context of rainfall-runoff model to produce flow at a downstream location from information at an upstream location, the present study uses ANN in a unique manner to predict discharges at the recession limb of the hydrograph from information at the rising limb of the same hydrograph. Thus, this paper will demonstrate somewhat a different application of ANN modelling to forecast flows in the Blue Nile. The developed ANN accuracy was further tested against prediction from an autoregressive model commonly used to model flow in recession period of a flow hydrograph.

2. Study area and data

El-Deim gauging station lies just over the border in the Sudan on the Blue Nile River (Fig. 1). The gauging station, which has the longest and most reliable record (Conway (1997); Sutcliffe and Parks (1999)), represents the outlet of an upper Blue Nile catchment of 350km² in the Ethiopian Plateau. The mean annual discharge at El-Deim station is 49 km³ for the period 1921-1990, ranging from a minimum of 31 km³ (1972 and 1984) to a maximum of 70 km³ (1929). Rainfall seasons in the Ethiopian Plateau is divided by the National Meteorological Services Agency (NMSA), in Ethiopia, into rainy season (June to September), dry season (October to January), and short rainy season (February to May). The short season rains, originating from the Indian Ocean, are brought by the south-east winds, while the heavy rains in the wet season originate from the Atlantic Ocean with the south-west winds (Tekleab et al. (2010); BCEOM (1999); Yilma and Ulrich (2004)).

10-day mean discharges at El-Deim gauging station have been obtained from the Ministry of Irrigation of the Sudan for 40 years (1961-2000). The data is arranged in 36 10-day mean discharges (as shown in Fig. 2 above) for 40 years. Discharges from period Q1Jun to Q1Oct (cf. Fig. 2) are selected to use as potential input data to the proposed ANN scenario models, whereas each discharge in the period Q2Oct to Q3May (cf. Fig. 2) is one of the required 23 outputs of the model that will be used for the operation of the Roseires Reservoir.

3. Methodology

3.1 Artificial Neural Network model used

Artificial Neural Network (ANN) is normally regarded as a non-linear multiple-input multiple-output black-box model. Inspired by the research into biological neural networks, the network receives an array of inputs and likewise produces an array of outputs. In the process of transformation of the inputs array to the outputs

array the neural network doesn't make any prior assumption about the specific mathematical functional form of relationship between the inputs and the outputs. Their use has recently grown, in different disciplines of sciences, as they provide solutions to complex modelling problems in different fields of science.

For more information on ANN and its used in modelling readers' attention is directed to the following sources (e.g. McCulloch and Pitts (1943); Hebb (1949)). The coming paragraphs are limited to description of the ANN model used in this study.

The Multi-Layer Feed Forward Network (MLFFN) type of ANN (also known as Wards nets as depicted in Fig. 3 below), which has dominated applications of neural networks in hydrological modelling (cf. Dawson & Wilby (2001); Maier & Dandy (2000)), is used in this study. It is characterized by its powerful capabilities in the modelling of complex nonlinear input output relations. It is simply a network of interconnected computational elements, i.e. the neurons, linked together by connection pathways, which are arranged in a series of layers, or slab (cf. Fig. 3), each layer performing a distinctive function in the operation of the network. The neuron layers of the MLFFN are the input layer, the output layer, and at least one hidden layer between the input and output layers. The input layer receives the external input array to the network, each input array element being assigned to only one neuron. The elements of the external input array are those time series used as input to the model. The output of each neuron in the input layer, which is equal to its external input element (corresponding to a unit or identity transformation), then becomes the input to the neurons in the hidden layer. Thus, each neuron in the hidden layer has an input array consisting of the outputs of the input layer neurons.

In this study, after extensive trials, two hidden layers (upper and lower) are used. Each hidden layer neuron produces only a single output which becomes an element of the input array to each neuron in the subsequent (output) layer. The final output Y_k is obtained by the following equation:

$$Y_k = S_1 \left\{ \left(\sum_{m=1}^M W_m S_2 \left(\sum_{i=1}^I W_i X_i + b_m \right) \right) + \sum_{j=1}^J W_j S_3 \left(\sum_{i=1}^I W_i X_i + b_j \right) \right\} + b_k \quad (1)$$

where,

Y_k The output from the network.

X_i The input to the network.

W_i The connection weights between nodes of the input and upper hidden layer.

W_j The connection weights between nodes of the input and lower hidden layer.

W_m The connection weights between nodes of the two hidden layers and output layer.

b_j, b_m & b_k are neuron thresholds (or baseflow) in the upper hidden, lower hidden, output layers, respectively.

S_2, S_3 & S_1 are transfer or activation functions for the upper hidden, lower hidden, output layers, respectively.

In the present flow forecasting context, the output layer has 23 neurons, which produce the final network output. The required number of neurons for the input and output layers is usually found from the number of pre-determined independent input variables (predictors) available and the number of dependent output

variables (predictand) required, respectively. However, the optimum number of neurons in each hidden layer is found by trial and error during the modelling process.

For all hidden and output layer neurons, the process of transformation of the input array to a single output is quite similar. In contrast to the simple unit-identity transformation used for the input layer neurons, this process is basically a nonlinear transformation of the total sum of the products of each of its input array elements with its corresponding weight, plus a constant "or baseflow" term known as the neuron threshold value as stated in equation 1 above. The function used in such transformation are known as the neuron transfer function. Three different transfer functions are used for the two hidden and output layers neurons. These are:

- *Gaussian Transfer Function (GTF)* in the upper hidden layer. The function produces output between 0 and 1 and has the following functional form:

$$f(x) = \exp(-x^2) \quad (3)$$

- *Gaussian Complement Transfer Function (GCF)* in the lower hidden layer. The function produces output between 0 and 1 and has the following functional form:

$$f(x) = 1 - \exp(-x^2) \quad (4)$$

- *Logistic Transfer Function (LOG)* in the output layer. The function produces output between 0 and 1 and has the following functional form:

$$f(x) = 1/(1 + \exp(-x)) \quad (5)$$

The weights and the threshold values constitute the parameters of the network, which are usually estimated by calibrating (or training) of the network. This is done by minimizing the sum of the squares of the differences between the network output series (Y_k), and the corresponding observed discharges, Q_i , using nonlinear optimization algorithms. In the present research, the software NeuroShell2 was used for building and calibrating the flow forecasting scenario models proposed.

3.2 Scenario models tested

The 10-day mean discharge data from El-Deim Station for the period 1960-2000 were used for building two scenario models (SM) based on different input variables. Each of the two models built is tested with different number of neurons in the hidden ANN layers. All four scenario models tested (hereinafter referred to as SM11, SM12, SM21 and SM22) have common output variables, which are the 23 10-day mean discharge during recession period. These are: Q2Oct, Q3Oct, Q1Nov, Q2Nov, Q3Nov, Q1Dec, Q2Dec, Q3Dec, Q1Jan, Q2Jan, Q3Jan, Q1Feb, Q2Feb, Q3Feb, Q1Mar, Q2Mar, Q3Mar, Q1Apr, Q2Apr, Q3Apr, Q1May, Q2May, and Q3May. As well as using 10-day mean discharge from months in the rising limb of the hydrograph, 10-day volume is also used as input variable (i.e. V1Jul and V1Aug in scenario models SM11 and SM12, see Table 1) to get the best possible forecasting model for discharges during the recession period. The input variables are chosen from the rising limb of the flood hydrograph to give ample lead time (a minimum of two months) before the first period required in the recession period. Table 1 show a summary for features of the scenario models tested.

As mentioned above, the software NeuroShell2 is used as a modelling tool in this study. The software is produced by Ward System Group that has developed its first neural network software in 1982 (cf. NeuroShell2 Website). It has options for beginner and advanced neural networks, as well as runtime facilities for creating runtime versions of trained networks and producing results files. In the scenario models tested in this study, 10% of the data series (four water years 1964/65, 1968/69, 1969/70 and 1991/92) has been used for testing purpose (to improve the network ability to generalize) and the rest 90% of the data series is used for training process.

3.3 Evaluation of model performance

3.3.1 Nash-Sutcliffe Efficiency

Performance of the models developed in this paper is evaluated using the well-known R^2 model efficiency criterion suggested by Nash and Sutcliffe (1970). This criterion is closely linked to the least-squares objective function being expressed as the sum of the squares of the differences F between the simulated discharge q_i and observed discharges Q_i . The R^2 model efficiency criterion can be expressed mathematically as:

$$R^2 = \frac{F_o - F}{F_o} \quad (6)$$

where,

$F = \sum (Q_i - q_i)^2$ with Q_i is the observed discharge and q_i is the corresponding simulated discharge and F_o is the initial sum squares of differences given by $F_o = \sum (Q_i - Q_o)^2$ with Q_o being the average of the observed discharge of the chosen training or the overall period.

The initial sum of squares of errors F_o can be viewed as a measure of performance of a primitive model producing a constant estimated discharge equal to the average of the observed discharge in the training or overall period. Thus, the R^2 criterion is, in essence, a global measure of the performance of the substantive model relative to that of the primitive model.

3.3.2 Mean Square Error

The error function is the function that is minimized during training. The mean squared error (MSE) function is most commonly used, although other error functions have also been proposed in literature. The advantages of using the MSE include that it is calculated easily, that it penalises large errors. It is given by:

$$MSE = \frac{1}{N} \sum_{i=1}^N (Q_i - q_i)^2 \quad (7)$$

where,

Q_i and q_i are as previously defined and N is the number of data values used.

This error will lead to the direction of the correct answers. Eventually, if the problem can be learned, a stable set of weights adaptively evolves and will produce good answers for all sample decisions or predictions.

3.4 Autoregressive model of the recession curve

In order to check accuracy of the model developed in this study, results from the model are compared to those obtained from an autoregressive model for the recession curve of the Blue Nile hydrograph. An autoregressive time series model for recession curve has been used for this purpose. In an extensive review for baseflow recession analysis methods and models, Tallaksen (1995), mentioned that autoregressive process is one of the successful models used for modelling recession curve or baseflow contribution in rivers. A first-order autoregressive model AR1 for a recession curve can be defined as:

$$Q_{t+l} = kQ_t + e_{t+l} \quad (8)$$

where e_t are assumed independent normally distributed errors with zero mean and constant variance; and k is a constant. This model was used by James and Thompson (1970) and Vogel and Kroll (1991) for modelling baseflow recessions and found successful, hence it was chosen to use here as a comparison model to gauge accuracy of the ANN model developed in this study. The recession curve or baseflow is considered in this study to be the flow period between Q1Oct to Q3May in Fig. 2.

4. Results and Discussion

The ANN model structure used here requires specification of number of neuron in the two hidden layer. This number is usually not known a priori, and was determined by a trial-and-error procedure in which the model is trained in succession with an increasing number of hidden neurons until reaching the optimum number of neurons. The optimum number of neurons in the hidden layers obtained for each is presented in Table 1 above.

Table 2 included performance results for the scenario models (SM) tested in terms of R^2 for the training, testing and overall periods, together with performance of the AR1 model. Generally, all four ANN scenario models tested are found very good, judging by the high values of R^2 values obtained for their performance for all modelled discharges. However, the results in Table 2 also indicate that accuracy of each scenario model is sensitive towards its inputs and the number of neurons in hidden layers. The effect of number of inputs is found more significant than the number of hidden neurons. The increase in number of input from four to five shows significant improvement in overall performance of models SM21 and SM22 in comparison to models SM11 and SM12 for all modelled discharges. However all scenario models performed well in modelling the 10-day discharges in the middle of the recession period than at its beginning and end.

Figs 4.1 and 4.2 show plots of the MSE for the scenario models in Table 1. In accordance with model performance in predicting discharge, the mean square error tends to be bigger for the modelled discharges at the beginning (cf. Fig. 4.1) and the end (cf. Fig. 4.2) of the recession period and smaller for the modelled discharges in the middle of the recession period.

Although the size of data used in building these models is relatively small and the number of modelled discharges (outputs) is too large (23 10-day mean discharges), however performance results of all models are found very rewarding and efficient in modelling the required discharges.

Based on the R^2 values for the testing period for the scenario models tested (cf. Table 2), coupled with the values of the MSE in Figs 4.1 & 4.2, scenario model SM21 is found to consistently perform better (in terms of higher positive values of R^2 and lower values of MSE) than the other three scenario models, although its overall performance R^2 values are similar to those of scenario model SM22. Therefore, scenario model SM21 is considered here as the optimum ANN model for forecasting the 23 discharges during the recession period of El-Deim flows that would be used as inflow to the Roseires Reservoir to estimate required storage, which subsequently be utilised in estimating irrigation water supply.

Simulated discharges from scenario model SM21 are further compared with those simulated by a first order autoregressive model (**AR1**) for the recession period in El-Deim flow hydrograph. The recession period considered here is the period from Q1Oct to Q3May. The statistical software SPSS from IBM is used to fit the AR1 in this study.

Comparative plots of the simulated discharges from scenario model SM21 and the AR1 model against the observed discharges of the 23 modelled discharges are shown in Figs 5.1 – 5.23. Visual comparison of the plots in Figs 5.1 – 5.23 shows there is a good match between the observed discharge and the discharge simulated by the scenario model SM21 for the overall period of data for all modelled discharges. In most cases an exact agreement between the observed and simulated discharges occurs during the whole modelling period. The only exceptions are one or two years for April and May discharges where there was an apparent disagreement resultant of the water year being relatively dry.. The overall performance of the ANN model is very high (>60%) indicating that the developed model is a good representation for the relation between discharges in the rising limb of the hydrograph and those in the falling limb of the same hydrograph.

Comparison of the discharges simulated by the developed model SM21 with those simulated by the AR1 model for the recession curve shows that the SM21 model out performs the AR1 model in producing discharges much closer to the observed ones.. The AR1 model tends to over-estimate or under estimate the observed discharges, especially at the tail of the recession curve (i.e. Q1Mar, Q2Mar, and Q1Apr).

Therefore based on this visual evidence, in addition to model performance criteria presented earlier, the ANN models developed in this study are better than the AR1 model or the graphical method currently used. Despite ANN models being classified as black box models and their outcomes can change if there is any physiographic change in the upstream catchment, however based on the above comparative results they can be recommended for use in the current situation.

5. Conclusions

This paper addresses the issue of modelling inflows to the Roseires Reservoir from outflows of El-Deim gauging station during the recession period of the Blue Nile in the Sudan. Lead time forecast of inflows to the Roseires Reservoir is needed for the operation of the Reservoir for irrigation water management and planning of cultivation area with cash crops (e.g. Cotton, Wheat, Sorghum, etc.).

Four Multi-Layer Feed-Forward Artificial Neural Network scenario models were proposed and tested. Different scenarios of inputs information and ANN structures have been tested to forecast 23 10-day mean discharges during the recession period. The application of ANN models in this study is considered unique as inputs to the models are taken from the rising limb of hydrograph (period 1st June to 10th October) of the water year and the outputs are the multi-discharges in the recession limb of the same hydrograph (period 20th October to 31st May). Using a 10-days mean discharge for the period 1961-2000, the four proposed models were trained and their performance were gauged using Nash-Sutcliffe R^2 and Mean Square Error (MSE).

The study found that both inputs and number of hidden neurons can affect the network forecasting ability. However, the number of input neurons has stronger effects than the number of hidden neurons. All developed models were found to perform very good in modelling the 23 discharges during the recession period of the Blue Nile. However, one model, which is referred in the study as scenario model SM21, was found to perform more superior and more accurate than the other three models and hence considered as the best model. Simulated discharges with model SM21 were compared to simulated discharges obtained by an AR1 model for the recession hydrograph to gauge its accuracy and found to perform better than the AR1. Therefore the model developed in this study is recommended for use, with reasonable confidence, to give lead time (2 months) forecast of the 10-day discharges in the period 20th October to 31st May, which would be used as inflows to the Roseires Reservoir. These more accurate (than those of the graphical method currently used by the Ministry of Irrigation in the Sudan) inflows would lead to better assessment for the future irrigation water supply and hence better water management in the Roseires Reservoir.

Acknowledgment

The authors would like to acknowledge the help received from Directorate of the Nile Water, in the Ministry of Irrigation of the Sudan in forms of data received and discussion taken place during the period of this study.

References

Abdellatif, M. (2004) “*Operation of Roseires and Sennar Dams Using Artificial Neural Network*”. Thesis (MSc), University of Khartoum, Sudan.

Abrahart, R. J., Heppenstall, A. J. & See, L. M. (2007) “*Timing error correction procedure applied to neural network rainfall–runoff modelling*”. Hydrol. Sci. J. 52(3), 414–431.

- Antar, A. M., Ellassiouti, I. & Allam, M. N. (2005) “*Rainfall–runoff modelling using artificial neural networks technique: a Blue Nile catchment case study*”. *Hydrol. Process.* 20(5), 1201–1216.
- BCEOM (1999) “*Abay Basin Integrated master plan study*”. Main report Ministry of Water Resources, Addis Ababa, Phase two, Volume, Agriculture, 1–2.
- Boucher, M. A., Perreault, L. & Anctil, F. (2009) “*Tools for the assessment of hydrological ensemble forecasts obtained by neural networks*”. *J. Hydroinform.* 11(3–4), 297–307.
- Chang, F.-J. & Chen, Y. C. (2001) “*A counterpropagation fuzzy-neural network modelling approach to real time streamflow prediction*”. *J. Hydrol.* 245(1–4), 153–164.
- Conway, D. (1997) “*A water balance model of the Upper Blue Nile in Ethiopia*”. *Hydrological Sciences Journal* 42, 265–286.
- Coulibaly, P., Anctil, F. & Bobe´ e, B. (2000) “*Daily reservoir inflow forecasting using artificial neural networks with stopped training approach*”. *J. Hydrol.* 230(3–4), 244–257.
- Dawson, C. W. & Wilby, R. L. (2001) “*Hydrological modelling using artificial neural networks*”. *Prog. Phys. Geogr.* 25(1), 80–108.
- Dawson, C. W., See, L. M., Abraham, R. J. & Heppenstall, A. J. (2006) “*Symbiotic adaptive neuro- evolution applied to rainfall–runoff modelling in northern England*”. *Neural Networks* 19(2), 236–247.
- Dibike, Y. B. & Solomatine, D. P. (2001) “*River flow forecasting using artificial neural networks*”. *Phys. Chem. Earth Part B Hydrol. Ocean. Atmos.* 26(1), 1–7.
- Hebb, D.O. (1949) “*The Organization of Behaviour*”. New York: John Wiley & Sons.
- James, L.D. and Thompson, W.O., (1970) “Least squares estimation of constants in a linear recession model”. *Water Resour. Res.*, 6(4): 1062-1069.
- Maier, H. R. & Dandy, G. C. (2000) “*Neural networks for the prediction and forecasting of water resources variables: a review of modelling issues and applications*”. *Environ. Model. Softw.* 15, 101–124.
- McCulloch, W.S. & Pitts, W. (1943) “*A Logical Calculus of the Ideas Immanent in Nervous Activity*”. *Bulletin of Mathematical Biophysics*, Vol 5.
- Nash, J. E. & Sutcliffe, J. V. (1970) “*River flow forecasting through conceptual models*”. *Part 1: a discussion of principles*. *J. Hydrol.* 10, 282–290.
- NeuroShell2 Website, (2012) “<http://wardsystems.com/neuroshell2.asp>”. Last accessed on 24/09/12.
- Pramanik, N. & Panda, R. K. (2009) “*Application of neural network and adaptive neuro-fuzzy inference systems for river flow prediction*”. *Hydrol. Sci. J.* 54(2), 247–260.
- Rajurkar, M. P., Kothiyari, U. C. & Chaube, U. C. (2004) “*Modelling of the daily rainfall–runoff relationship with artificial neural network*”. *J. Hydrol.* 285(1–4), 96–113.
- Shamseldin, A. Y. (1997) “*Application of neural network technique to rainfall–runoff modelling*”. *J. Hydrol.* 199, 272–294.
- Shamseldin, A. Y. (2010) “*Artificial neural network model for river flow forecasting in a developing country*”. *Journal of Hydroinformatics*, 12.1.

- Shamseldin, A. Y., Nasr, A. E. & O'Connor, K. M. (2002) “*Comparison of different forms of the Multi-layer Feed-Forward Neural Network method used for river flow forecast combination*”. J. Hydrol. Earth Syst. Sci. 6(4), 671–684.
- Shamseldin, A. Y., O'Connor, K. M. & Nasr, A. E. (2007) “*A comparative study of three neural network forecast combination methods for river flow forecasting*”. Hydrol. Sci. J. 55(2), 898–916.
- Sughaiyaroun, E, (1968) “Regulation Rules for the Working of the Reservoirs at Roseires and Sennar on the Blue Nile”. Ministry of Irrigation and Hydro-electric Power, The Republic of the Sudan, Khartoum, Sudan.
- Sutcliffe, J. V. and Parks, Y. P. (1999) “*The hydrology of the Nile*”. IAHS Special publication No.5 IAHS press, Institute of Hydrology, Wallingford, Oxfordshire.
- Tallaksen, L. M., (1995) “A review of baseflow recession analysis”. J. Hydrol. 165, 349-370.
- Tekleab, S., Uhlenbrook, S., Mohamed, Y., Savenije, H. H. G., Ayalew, S., Temesgen, M. and Wenninger, J. (2010). “*Water balance modeling of Upper Blue Nile catchments using a top-down approach*”. Hydrol. Earth Syst. Sci. Discuss 7, 6851–6886.
- Vogel, R.M, and Krotl, C.N., (1991) “Estimation of baseflow recession constants”. (Abstract) In: D.S. Bowles and P.E. O'Connell (Editors), Recent Advances in the Modelling of Hydrologic Systems. Proc. NATO Advanced Study Inst., Sintra, 1988. NATO ASI Series C, 345, Kluwer, Dordrecht, p. 659.
- Yilma, S. and Ulrich, Z. (2004) “*Recent changes in rainfall and rainy days in Ethiopia*”. Int. J. Climatology, 24, 973–983, doi:10.1002/joc.1052.

Table 1: Main features of the scenario models tested

Model Scenario	Input Variables	Number of Neurons in Hidden Layers		Transfer Functions Used		
		Upper Layer	Lower Layer	Upper Hidden	Lower Hidden	Output Layer
SM11	Q1Jun, Q1Oct, V1Jul, V1Aug.	30	25	GTF	GCF	LOG
SM12	Q1Jun, Q1Oct, V1Jul, V1Aug.	30	40	GTF	GCF	LOG
SM21	Q1Jun, Q1Jul, Q2Jul, Q1Aug, Q2Aug.	30	25	GTF	GCF	LOG
SM22	Q1Jun, Q1Jul, Q2Jul, Q1Aug, Q2Aug.	30	40	GTF	GCF	LOG

Table 2: Performance results, in terms of R^2 for the tested ANN and AR1 models

Modelled Discharge	SM11			SM12			SM21			SM22			AR1
	Training	Testing	Overall	Training	Testing	Overall	Training	Testing	Overall	Training	Testing	Overall	Overall
Q2Oct	0.99	0.30	0.96	0.99	0.15	0.96	0.99	0.88	0.98	0.99	0.11	0.91	0.56
Q3Oct	0.98	0.64	0.94	0.98	0.65	0.94	0.99	0.91	0.93	0.99	0.55	0.80	0.75
Q1Nov	0.99	0.08	0.90	0.99	0.77	0.96	0.99	0.84	0.89	0.99	0.45	0.74	0.69
Q2Nov	0.90	0.11	0.83	0.91	0.46	0.87	0.99	0.90	0.93	0.99	0.76	0.84	0.68
Q3Nov	0.92	0.52	0.90	0.95	0.36	0.91	0.99	0.96	0.98	0.99	0.14	0.92	0.85
Q1Dec	0.93	0.98	0.93	0.98	-0.28	0.91	0.99	0.92	0.96	0.99	0.69	0.98	0.76
Q2Dec	0.96	0.93	0.96	0.97	0.27	0.92	0.99	0.94	0.97	0.99	0.84	0.99	0.88
Q3Dec	0.99	0.77	0.97	0.99	0.70	0.97	0.99	0.98	0.99	0.99	0.02	0.89	0.72
Q1Jan	0.98	0.78	0.96	0.95	0.78	0.94	0.99	0.93	0.92	0.99	0.53	0.88	0.67
Q2Jan	0.97	0.65	0.95	0.96	0.74	0.94	0.99	0.88	0.94	0.99	0.17	0.92	0.56
Q3Jan	0.96	-0.33	0.87	0.96	-0.81	0.89	0.99	0.98	0.96	0.99	0.75	0.89	0.41
Q1Feb	0.99	0.63	0.96	0.97	0.64	0.95	0.99	0.98	0.96	0.99	0.27	0.91	0.61
Q2Feb	0.97	0.76	0.96	0.97	0.43	0.93	0.99	0.58	0.73	0.99	0.31	0.84	0.54
Q3Feb	0.97	0.41	0.94	0.95	-0.03	0.90	0.99	0.57	0.62	0.99	0.33	0.65	0.40
Q1Mar	0.97	-0.82	0.79	0.93	0.96	0.94	0.99	0.71	0.74	0.99	0.76	0.72	-0.29
Q2Mar	0.92	-0.05	0.74	0.74	0.76	0.78	0.99	0.87	0.93	0.99	0.43	0.73	-0.31
Q3Mar	0.93	0.77	0.88	0.21	0.73	0.50	0.99	0.85	0.94	0.99	0.20	0.57	0.19
Q1Apr	0.91	0.70	0.89	0.85	0.45	0.82	0.99	0.57	0.75	0.99	0.86	0.85	0.61
Q2Apr	0.94	0.68	0.92	0.99	0.50	0.95	0.99	0.20	0.39	0.99	0.38	0.87	-0.29
Q3Apr	0.93	-0.24	0.77	0.85	-0.49	0.65	0.99	0.36	0.48	0.99	0.16	0.88	0.27
Q1May	0.89	0.88	0.89	0.89	0.43	0.81	0.99	0.57	0.75	0.99	0.45	0.75	0.41
Q2May	0.95	-0.50	0.48	0.93	-0.49	0.81	0.99	0.58	0.76	0.99	0.41	0.49	0.26
Q3May	0.99	-0.82	0.73	0.99	0.54	0.99	0.99	0.86	0.93	0.99	0.45	0.98	0.20

Figure Caption

Figure	Title
Figure 1	Location map of the study area
Figure 2	The Blue Nile 10-day mean discharges at El-Deim station for a typical hydrological/water year
Figure 3	Multi-Layer Feed Forward NN of 2 Hidden Layers (slabs)
Figure 4.1	MSE from the tested scenario models for discharges Q2Oct to Q1Feb
Figure 4.2	MSE from the tested scenario models for discharges Q1Feb to Q3May.
Figure 5.1	Observed and simulated discharges with SM21 and AR1 for Q2Oct
Figure 5.2	Observed and simulated discharges with SM21 and AR1 for Q3Oct
Figure 5.3	Observed and simulated discharges with SM21 and AR1 for Q1Nov
Figure 5.4	Observed and simulated discharges with SM21 and AR1 for Q2Nov
Figure 5.5	Observed and simulated discharges with SM21 and AR1 for Q3Nov
Figure 5.6	Observed and simulated discharges with SM21 and AR1 for Q1Dec
Figure 5.7	Observed and simulated discharges with SM21 and AR1 for Q2Dec
Figure 5.8	Observed and simulated discharges with SM21 and AR1 for Q3Dec
Figure. 5.9	Observed and simulated discharges with SM21 and AR1 for Q1Jan
Figure 5.10	Observed and simulated discharges with SM21 and AR1 for Q2Jan
Figure 5.11	Observed and simulated discharges with SM21 and AR1 for Q3Jan
Figure 5.12	Observed and simulated discharges with SM21 and AR1 for Q1Feb
Figure5.13	Observed and simulated discharges with SM21 and AR1 for Q2Feb
Figure 5.14	Observed and simulated discharges with SM21 and AR1 for Q3Feb
Figure 5.15	Observed and simulated discharges with SM21 and AR1 for Q1Mar
Figure 5.16	Observed and simulated discharges with SM21 and AR1 for Q2Mar
Figure. 5.17	Observed and simulated discharges with SM21 and AR1 for Q3Mar
Figure. 5.18	Observed and simulated discharges with SM21 and AR1 for Q1Apr
Figure. 5.19	Observed and simulated discharges with SM21 and AR1 for Q2Apr
Figure 5.20	Observed and simulated discharges with SM21 and AR1 for Q3Apr
Figure 5.21	Observed and simulated discharges with SM21 and AR1 for Q1May
Figure 5.22	Observed and simulated discharges with SM21 and AR1 for Q2May
Figure 5.23	Observed and simulated discharges with SM21 and AR1 for Q3May

Figures

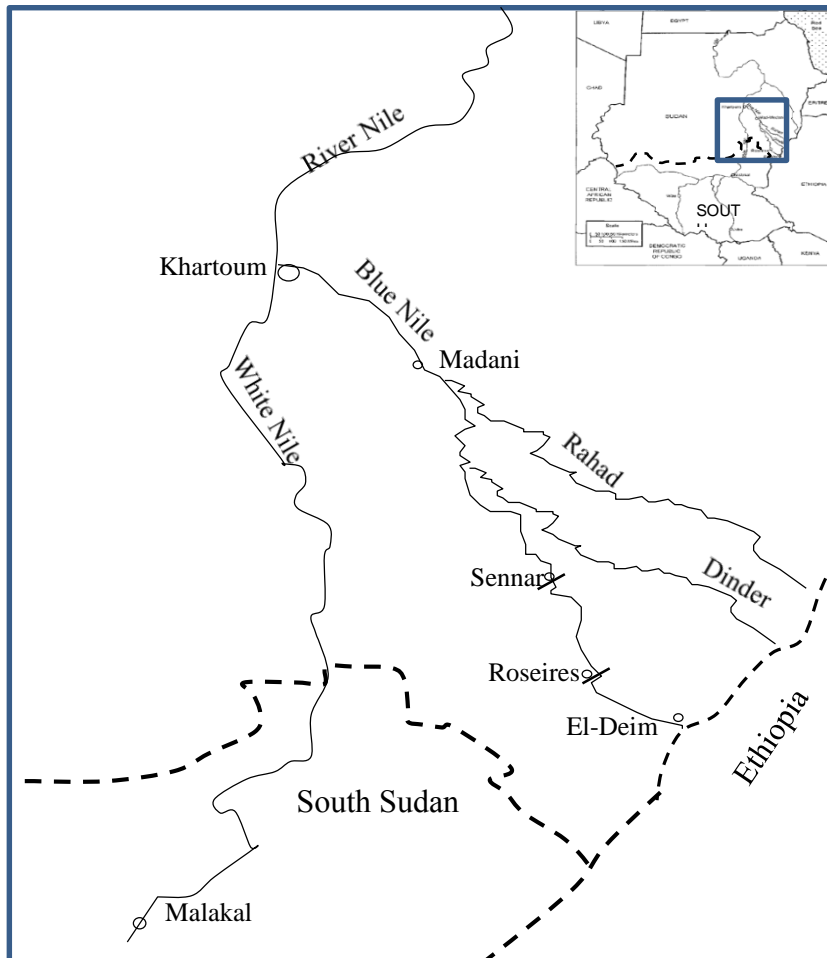


Figure 1

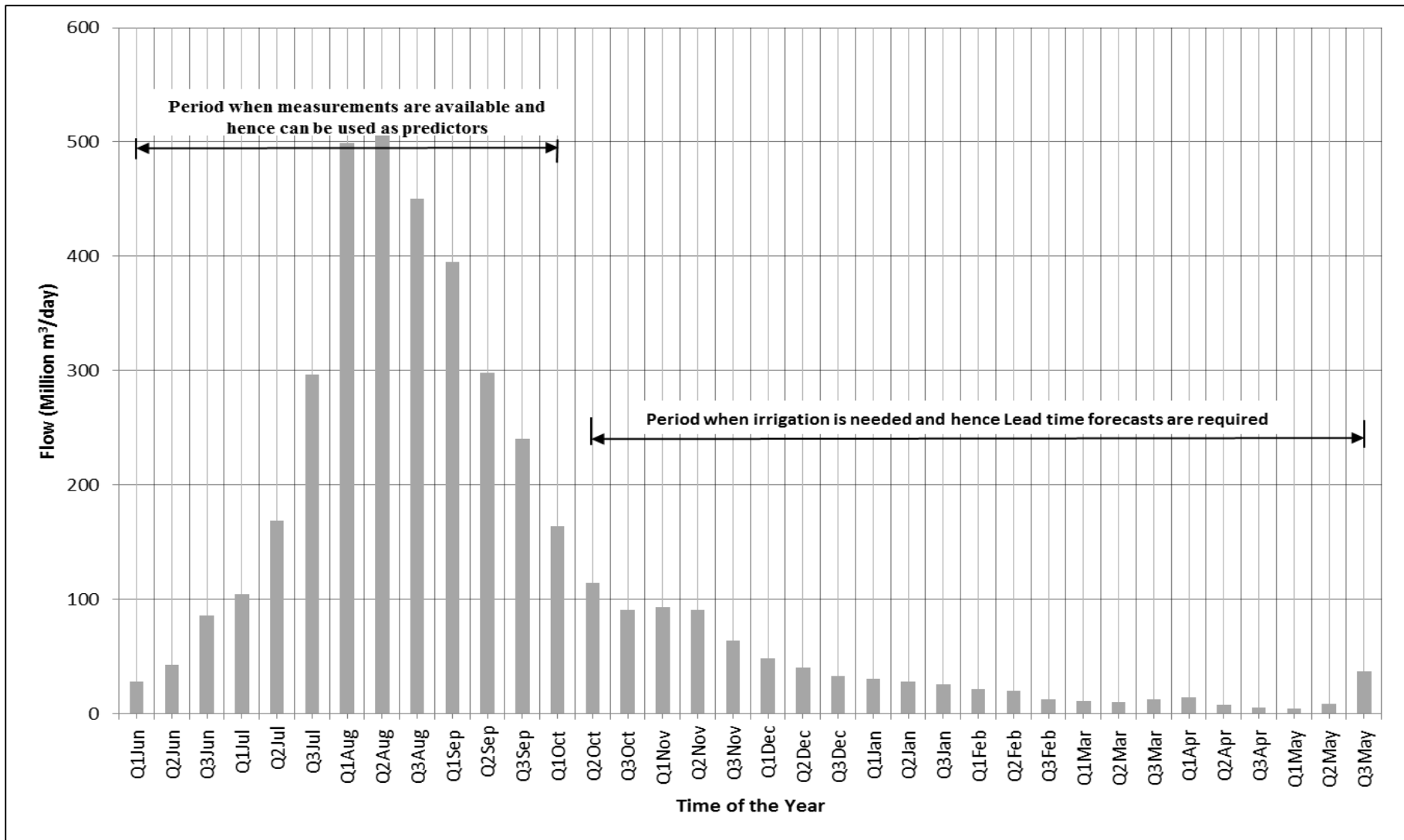


Figure 2

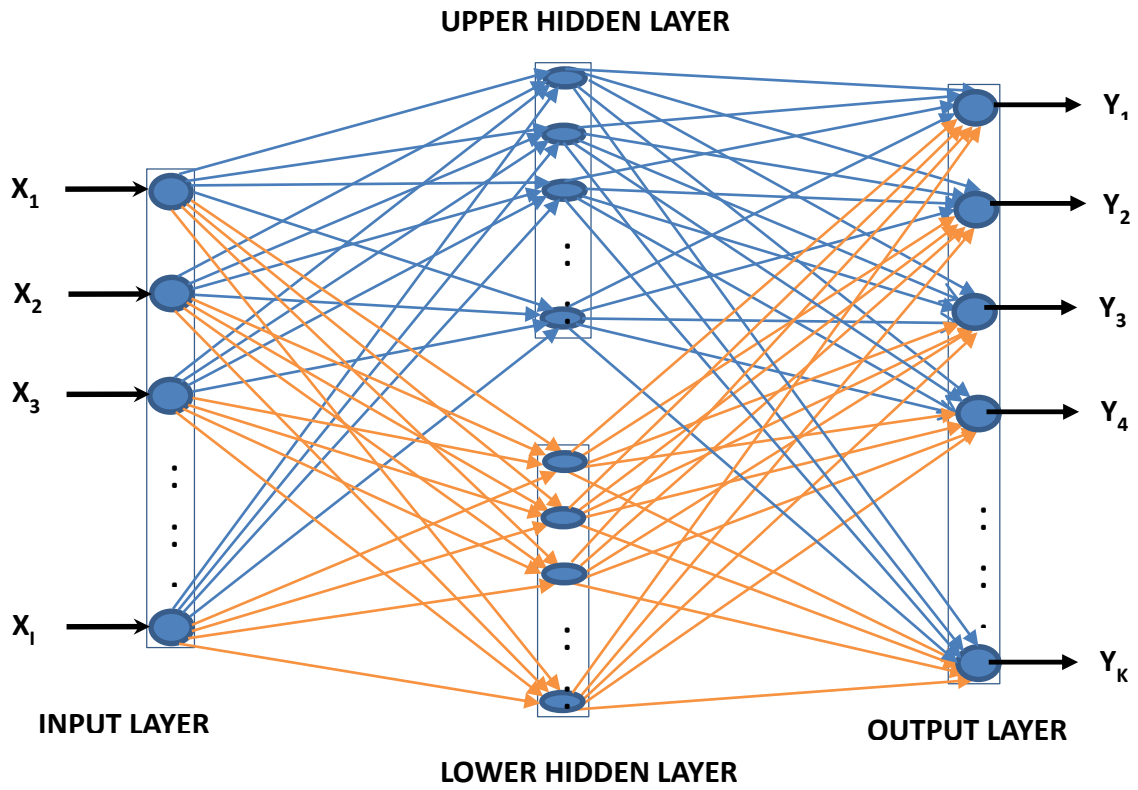


Figure3

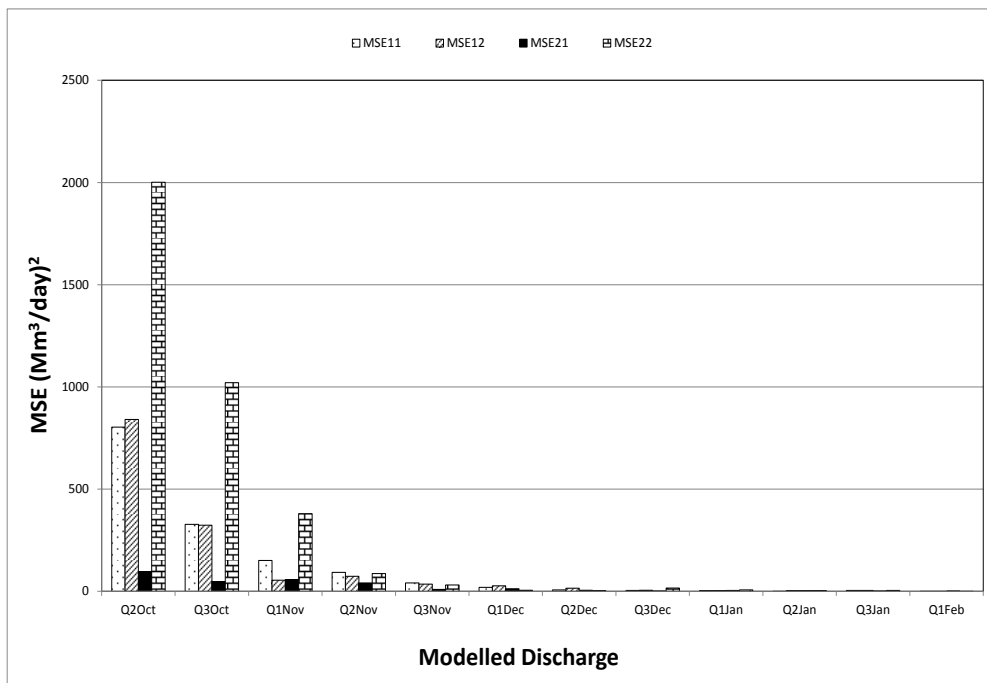


Figure 4.1

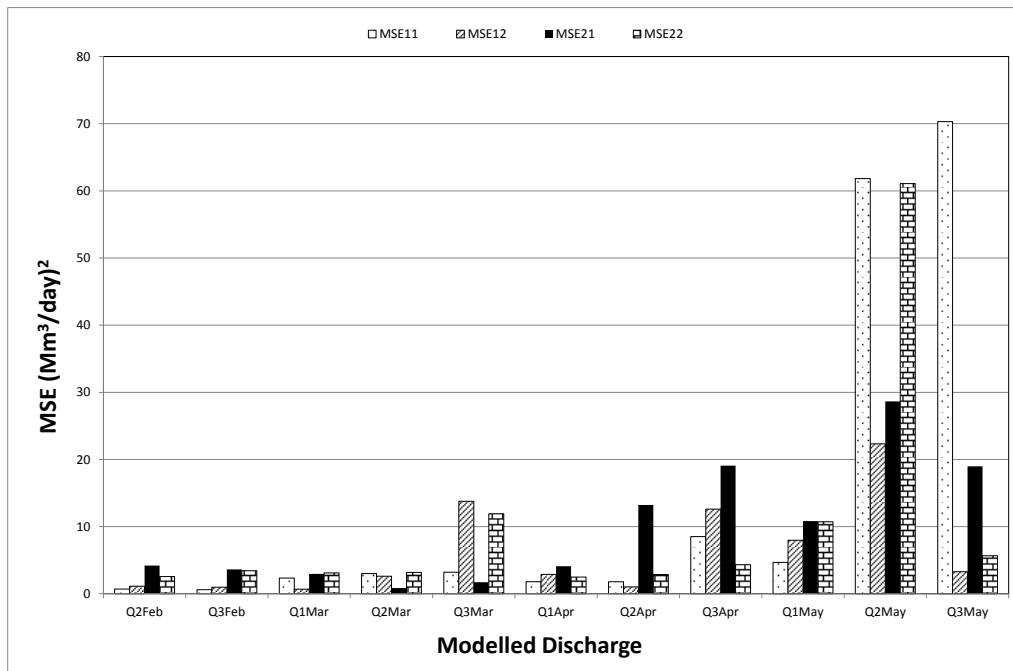


Figure. 4.2

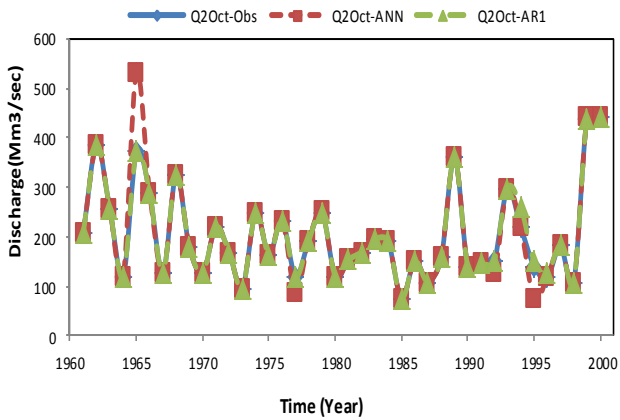


Figure. 5.1

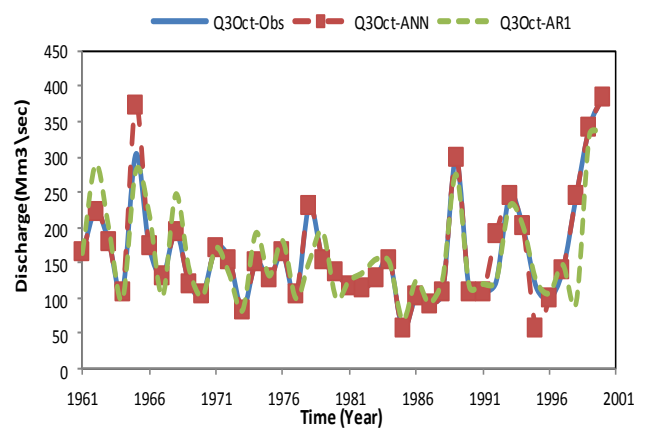


Figure. 5.2

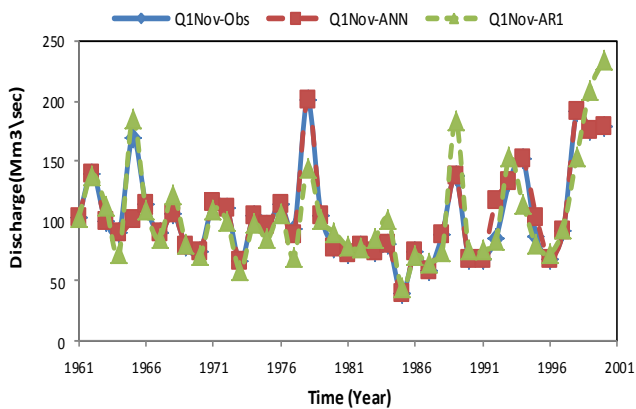


Figure. 5.3

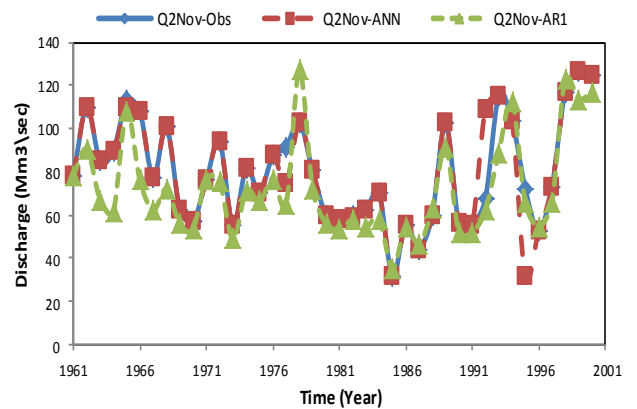


Figure. 5.4

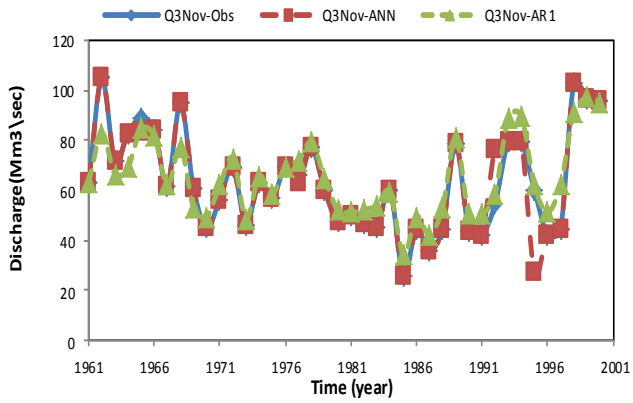


Figure. 5.5

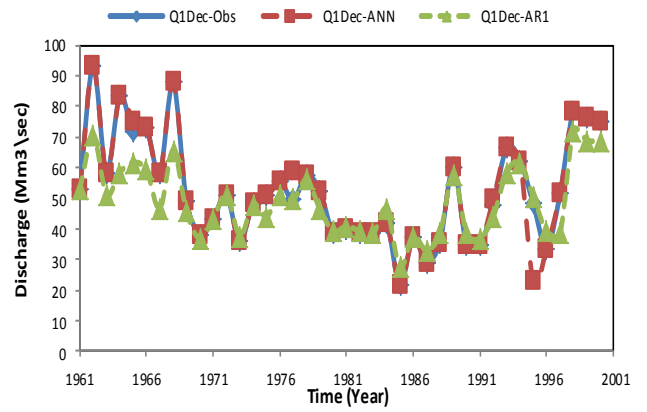


Figure. 5.6

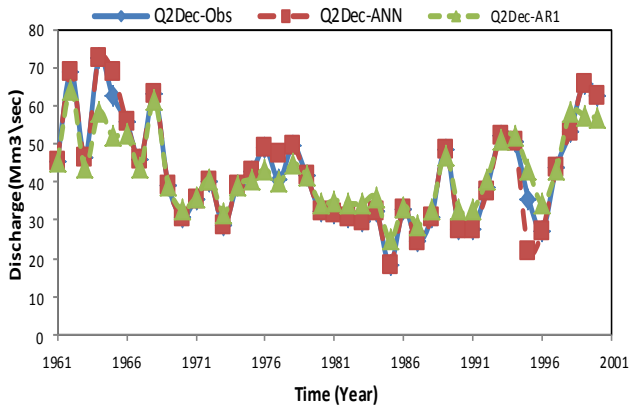


Figure. 5.7

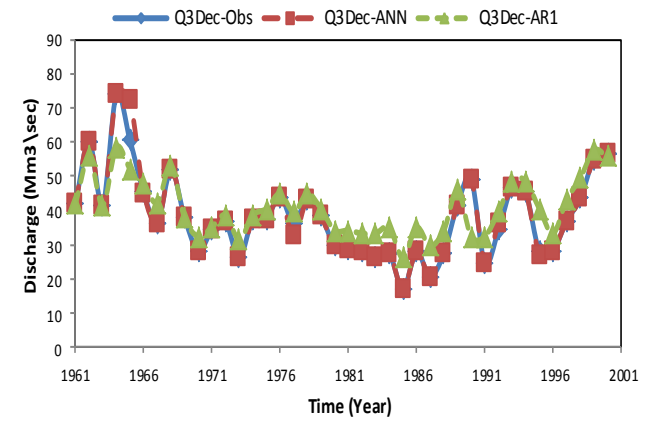


Figure. 5.8

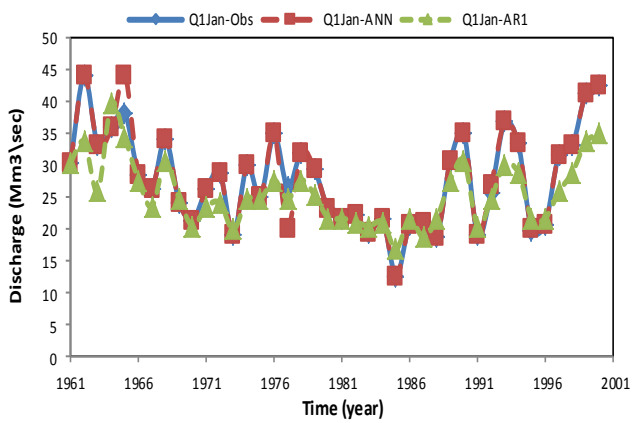


Figure. 5.9

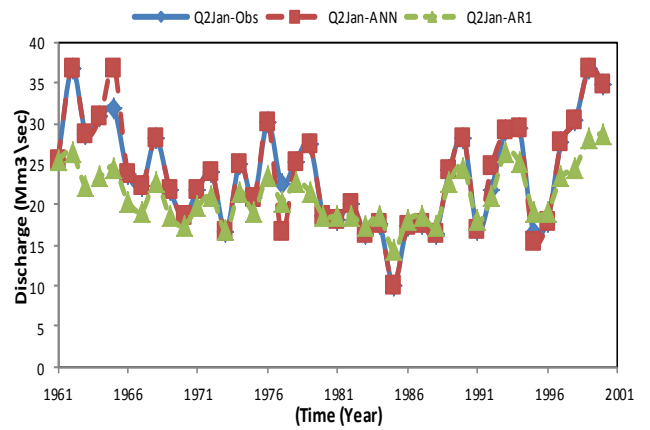


Figure. 5.10

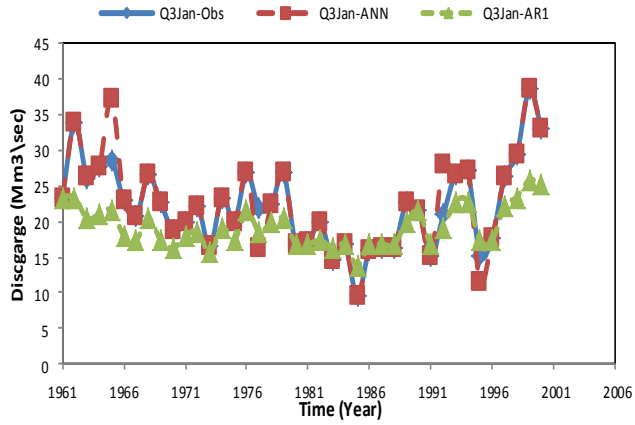


Figure. 5.11

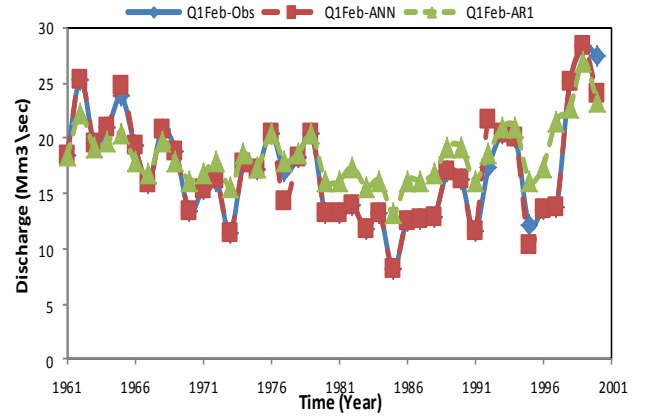


Figure. 5.12

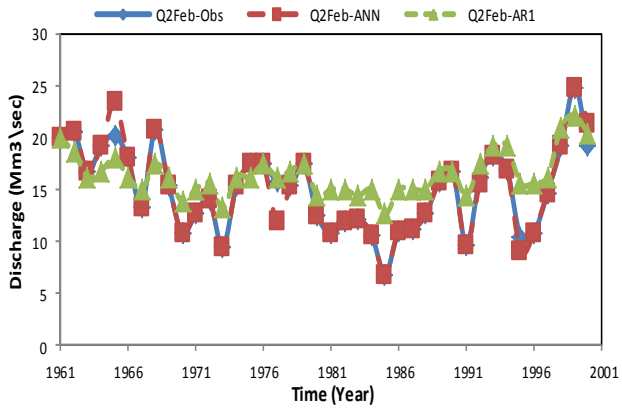


Figure. 5.13

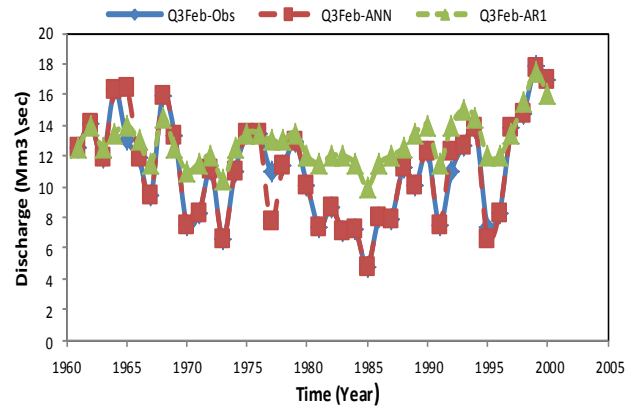


Figure. 5.14

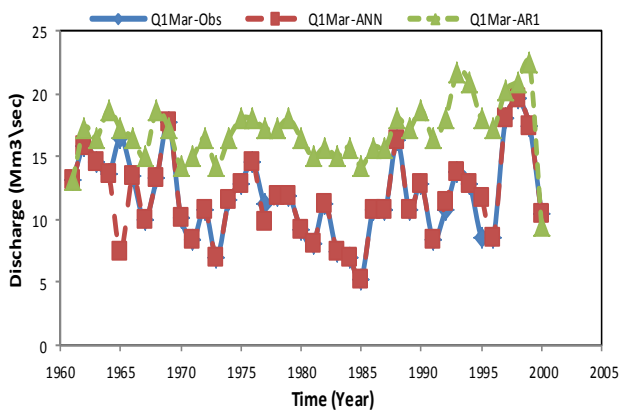


Figure. 5.15

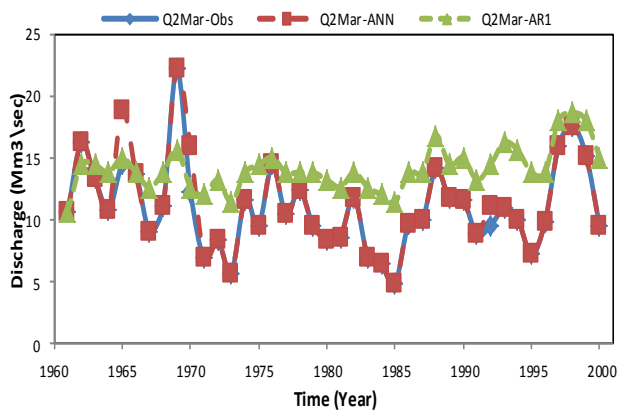


Figure. 5.16

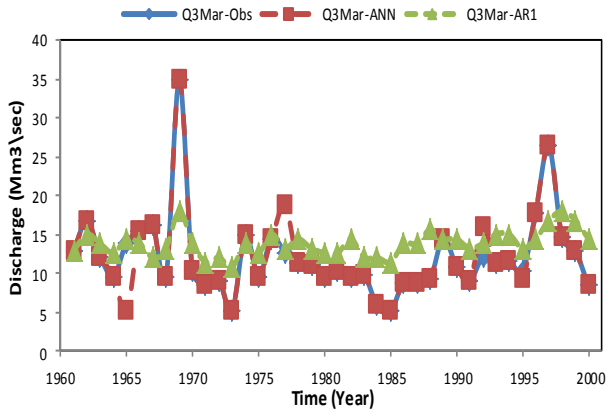


Figure. 5.17

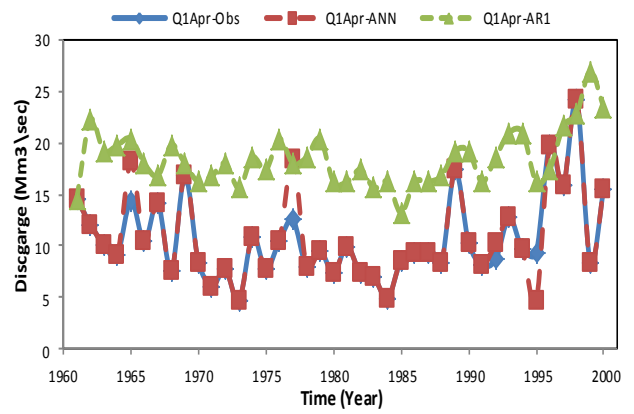


Figure. 5.18

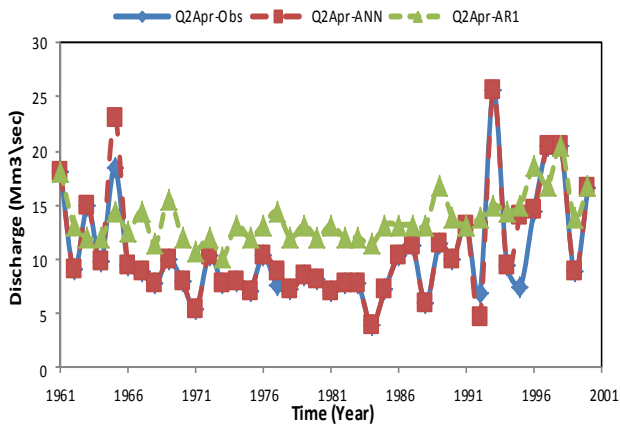


Figure. 5.19

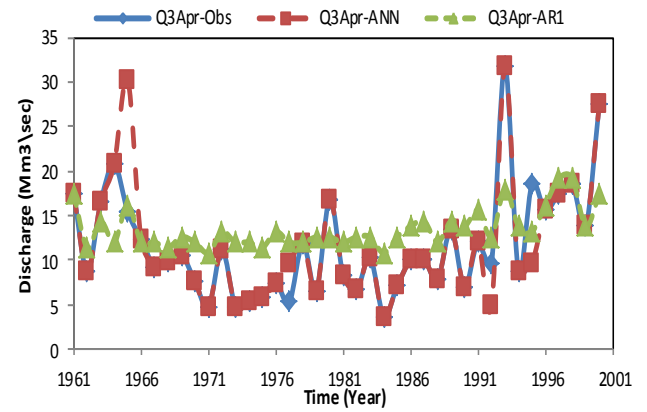


Figure. 5.20

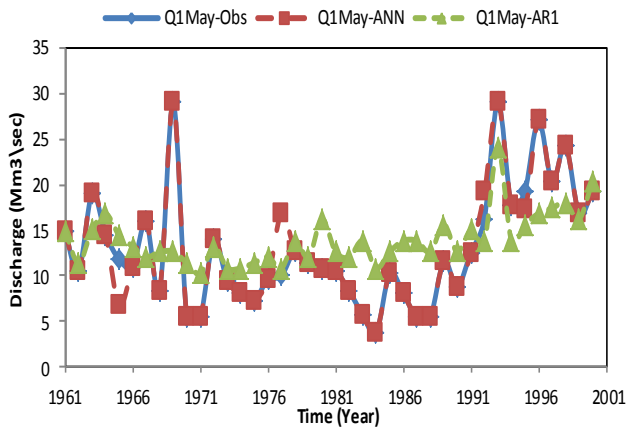


Figure. 5.21

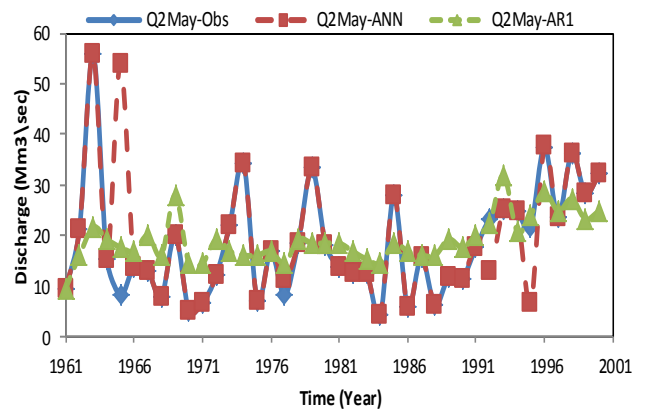


Figure. 5.22

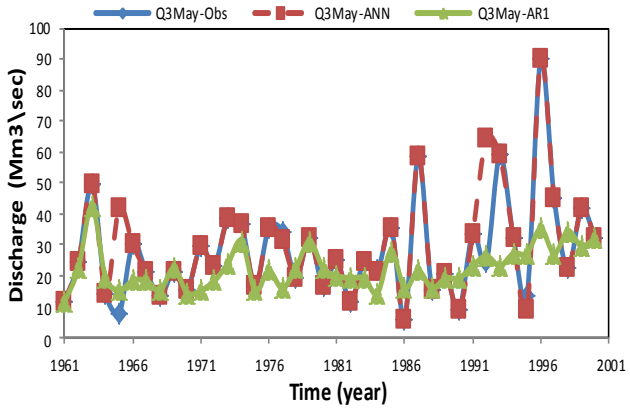


Figure. 5.23